Sources of Temporal Decorrelation in an Agricultural Scene and Their Effect on Sub-Daily Sar Coherence Time Series

Villarroya-Carpio, A.; Lopez-Sanchez, J. M.; Aguasca, A.; Broquetas, A.; Fabregas, X.; Mas, M.; Steele-Dunne, S.

DOI
10.1109/IGARSS53475.2024.10641969

Publication date
2024

Document Version
Final published version

Published in
IGARSS 2024 - 2024 IEEE International Geoscience and Remote Sensing Symposium, Proceedings

IGARSS 2024 - 2024 IEEE International Geoscience and Remote Sensing Symposium | 979-8-3503-6032-5/24/$31.00 ©2024 IEEE | DOI: 10.1109/IGARSS53475.2024.10641969

SOURCES OF TEMPORAL DECORRELATION IN AN AGRICULTURAL SCENE AND THEIR EFFECT ON SUB-DAILY SAR COHERENCE TIME SERIES

*A. Villarroya-Carpio, J. M. Lopez-Sanchez**

Institute for Computer Research
University of Alicante
Alicante, Spain

A. Aguasca, A. Broquetas, X. Fabregas, M. Mas

CommSensLab, Dept. TSC
Univ. Politècnica de Catalunya
Barcelona, Spain

S. Steele-Dunne

Dept. of Geoscience and Remote Sensing
TU Delft
Delft, The Netherlands

ABSTRACT

Data obtained during a ground-based SAR experiment and an associated field campaign have been exploited to study the rate and sources of decorrelation in an agricultural test site in the conditions of observation of a geosynchronous SAR. It was found that the scene is less affected by temporal decorrelation when the primary image is acquired during night time or early morning. Additionally, a periodic oscillation on a sub-daily scale was observed when creating coherence time series with increasing temporal baseline. Two factors which strongly contribute to these oscillations are the daily cycles of soil moisture and evapotranspiration.

Index Terms— Agriculture, Ground-based Synthetic Aperture Radar (GB-SAR), interferometric coherence, soil moisture, evapotranspiration

1. INTRODUCTION

The use of Synthetic Aperture Radar (SAR) data is becoming more widespread in the field of agriculture, due to its improved spatial resolution compared to passive microwave remote sensing and generally better temporal coverage than optical imagery, on account of not being affected by the presence of clouds [1].

In addition to observables derived from the measured backscattered intensity, SAR interferometry provides coherence and phase measurements related to the scene's vertical dimension and other properties [2]. In the context of agriculture SAR interferometry has been successfully exploited for the purposes of crop type mapping [3, 4, 5], retrieval of other biophysical variables [6, 7, 8], and crop monitoring [9, 10, 11].

In recent years there has been a growing interest in the availability of SAR imagery at increased temporal resolutions, particularly at sub-daily scales. In this line, different mission proposals have developed plans for sub-daily SAR observations, like Hydroterra [12], or the SLAINTE mission idea, recently submitted in response to the 12th call for ESA Earth Explorers [13]. A few studies have focused on the use of radar at sub-daily scales [14, 15].

This work has focused on exploiting data from the Hydrosoil campaign [16], which simulated the observation conditions (shallow incidence angles, sub-daily acquisitions, etc.) of the Hydroterra mission proposal over an agricultural area. The goal was to profit from the characteristics of this dataset in order to study the dynamics of SAR interferometry at sub-daily timescales. Given the availability of multiple temporal baselines, the first objective was to study the rate of decorrelation of an agricultural area at different moments during the season, as well as the effect of the choice of time of acquisition during the day. Secondly, the evolution of the interferometric coherence within a day was studied, particularly its sensitivity to soil moisture and daily dynamics of the vegetation.

2. DATASET AND METHODOLOGY

The Hydrosoil campaign consisted on an experiment carried out with a ground-based SAR system monitoring an agricultural field during eight months in 2020. The instrument acquired C-band full-polarimetric images every 10 minutes. Additionally, supplementary data regarding meteorological parameters, soil roughness and moisture and vegetation variables (plant density, LAI, height, and water content) were measured during the campaign. The campaign spanned the complete growing cycles of two different crops: barley and corn.

The research work described below was limited to the first season, corresponding to barley, and specifically focused on the repeat-pass interferometric coherence. Multiple coherence time series were constructed, differing in the way the interferograms were computed:

1. Long-term (seasonal) series:

*This work was supported in part by the the European Funds for Regional Development and by the Spanish Ministry of Science and Innovation (Agencia Estatal de Investigación, AEI) with Project PID2020-117303GB-C22/AEI/10.13039/501100011033.

- They span the entire season, with an interferogram every 10 minutes.
- Primary image changes for every interferogram.
- A specific temporal baseline is used for each of the series built in this way: 10 and 30 minutes, 1, 3, 6, 12 and 18 hours, and 1, 3, 6, and 12 days.

2. Daily-reset series:

   - Four series covering the entire season, with an interferogram every 10 minutes.
   - For each of the series the primary image resets daily at a specific time: 0:00, 6:00, 12:00, and 18:00.
   - The temporal baseline increases in 10-minute steps from the starting time until the primary image changes again.

3. Short-term series:

   - Four different time series for each date of the season.
   - Primary image fixed at 0:00, 6:00, 12:00 or 18:00 of the specific date.
   - The temporal baseline increases from 10 minutes to 12 days in 10-minute steps.

In summary, for the first set of series the interferograms are created with a "moving window" with a fixed width in each case. In the second set, the window moved once a day with the width progressively increasing. And in the final case, the start of the window was fixed in time while the width gradually increased.

The construction of these different time series aims to highlight the sources of both short and long-term temporal decorrelation. Soil moisture (SM) and daily cycles in the vegetation cover have been considered as the main sources of the short-term decorrelation, while changes in the phenology of the vegetation and other variables contribute to the loss of correlation in the long term.

The first point of interest has been to study the rate of decorrelation during different stages of the campaign and for different ranges of temporal baselines. Two simple functions [17] have initially been used to describe the temporal decorrelation:

$$\gamma(t) = \gamma_0 e^{-t/\tau} \tag{1}$$

$$\gamma(t) = (\gamma_0 - \gamma_\infty) e^{-t/\tau} + \gamma_\infty \tag{2}$$

where γ_0 is the initial coherence, which should be close to 1, γ_∞ is the long-term coherence, and τ represents the decorrelation rate.

Subsequently, a new periodic term was added to Eq. 2 in order to take into account the oscillations observed in the coherence time series for sub-daily temporal baselines:

$$\gamma(t) = (\gamma_0 - \gamma_\infty) e^{-t/\tau} + A e^{-t/\tau_2} \cos\left(\frac{2\pi}{T} t + \phi_0\right) + \gamma_\infty \tag{3}$$

where A represents the initial amplitude of the oscillation, τ_2 accounts for the potential attenuation of this term over time, ϕ_0 represents the initial phase of this oscillation, and T denotes the period, which is fixed to 1 day.

In an effort to assess the effect of the SM in the coherence time series, the in-situ SM data have been used to compute curves of simulated coherence. In [18], an empirical model to estimate the dielectric constant of the surface based on soil moisture data is presented. Furthermore, the model described in [19] was used to subsequently derive the complex interferometric coherence. The coherence magnitude obtained through this method has been compared to the coherence time series resulting from the measured data.

On the other hand, to account for the daily dynamics of vegetation, the vapour pressure deficit (VPD, [20]) has been calculated. It is a function of temperature and relative humidity, and is related to the rate of evapotranspiration of the vegetation.

3. RESULTS AND DISCUSSION

3.1. Varying temporal baselines and rate of decorrelation

Figure 1 shows three time series spanning the whole season corresponding to the coherence amplitude values obtained with different temporal baselines in the interferograms, as detailed in Section 2. The coherence values are estimated by averaging all the pixels within the whole field. In all 3 curves there is an overall downwards trend as the season advances, and the increasing presence of vegetation becomes the main source of temporal decorrelation in the scene. The sudden drops in coherence correspond to rain events. An increase in the temporal baseline in this case means that the effect of these events is "seen" by more interferograms. Finally, a daily ripple is observed, as the coherence is higher when the primary image is acquired at nighttime, when the scene is more stable.

The effect of increasing the temporal baseline, particularly on the decorrelation rate, has been studied quantitatively. Figure 2 shows the average coherence values resulting from keeping the same primary image and increasing the temporal baseline from 1 to 12 days. The decrease in the coherence amplitude can be described, as expected, by Eqs. 1 and 2. It was observed how, irrespectively of the moment of the season, the long term coherence remains clearly over 0, being the second model the most accurate description of the curves. In most cases HH experiences a slower decline than HV and VV.

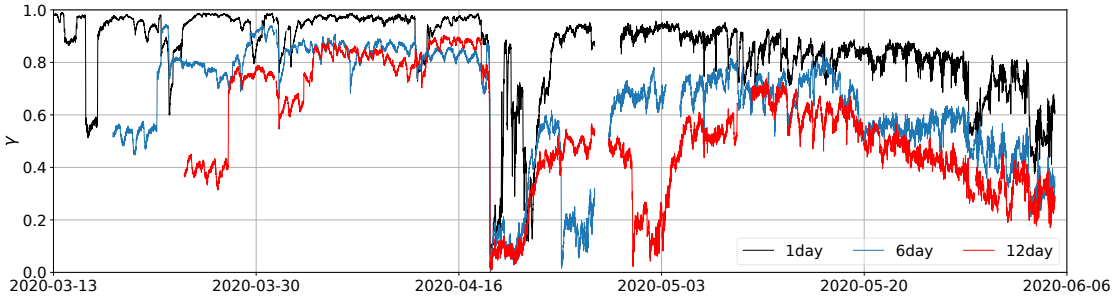

Fig. 1. Coherence time series (HH channel) for the barley season obtained with different temporal baselines: 1 day, 6 days, and 12 days. The x-axis displays the date for the secondary image.

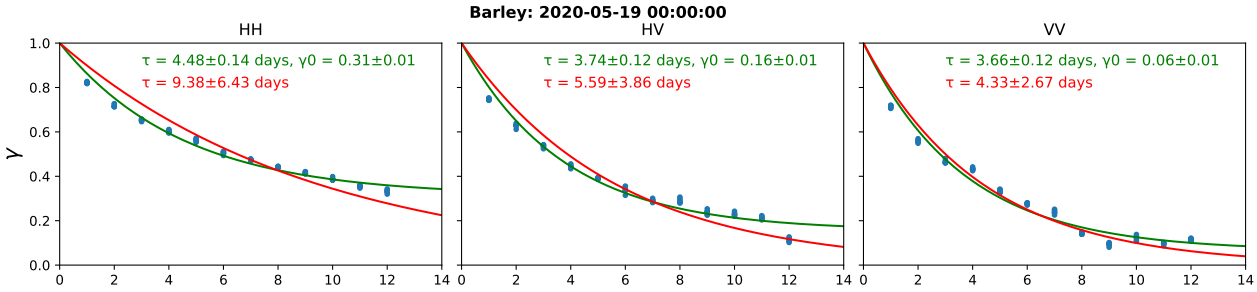

Fig. 2. Example of the decorrelation curves for the different polarimetric channels. The primary image is set, while the temporal baseline (in days) is increased. The fitting parameters obtained in the models of Eqs. 1 and 2 are shown.

When this analysis is extended to smaller temporal baselines, a new behaviour is observed: on top of the progressive decay of the coherence there is an oscillation (Figure 3), with a period of approximately one day, and time intervals where the coherence is partially recovered. This oscillation appears well defined when the chosen primary image is acquired at night time. In these cases, a plateau is observed around the 1-day temporal baseline, where the coherence remains high and approximately constant. This behaviour is not as clearly observed later in the season, due to the vegetation growth, or when the primary image is selected during the daytime, specially in the afternoon, since the vegetation and the atmospheric conditions experiment the most changes, including wind.

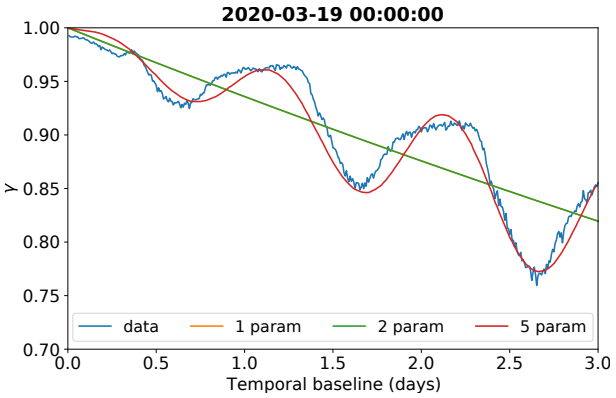

Fig. 3. Evolution of the coherence amplitude (HH channel) for temporal baselines between 10 minutes and 3 days. The curves obtained from the best fits of models in Eqs. 1, 2 and 3 are also represented.

3.2. Short-term temporal decorrelation and daily cycle

The first plot in Figure 4 shows the coherence time series for each polarimetric channel for the full growing cycle of the barley campaign. It covers from the beginning of the campaign until the date the crop is harvested. The daily ripple is caused by the reset of the primary image in the interferograms, while the more pronounced drops in the coherence correspond to rainfall events. Coherence decreases during the daytime and tends to partially recover at night, when the conditions of observation are more similar to those during the acquisition of the primary image, and when the scene experiments fewer changes. The amplitude of the oscillations in the coherence during the day increases later in the time series, showing the increasing effect of the dynamics of the vegetation in the short-term temporal decorrelation as the plants grow.

The second and third plots in Figure 4 display the mod-

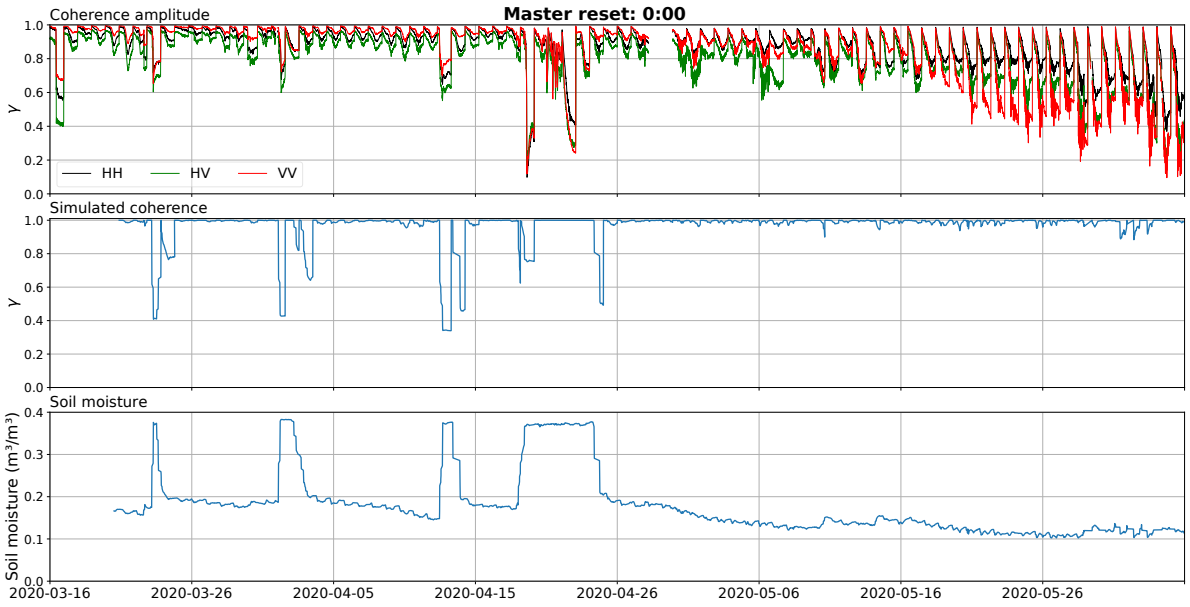

Fig. 4. Time series of measured coherence, simulated (modelled) coherence, and soil moisture for the whole growing season of barley.

elled coherence and the soil moisture data used to simulate it, respectively. The sudden increases in the SM reflect the rain events. The SM curve presents daily oscillations and a downward trend after each period of rainfall. The simulated coherence replicates these oscillations and shows sharp drops matching the increase and decrease of soil moisture associated with rain events.

Despite the measured and the simulated coherence sharing the more pronounced peaks, the amplitude of the oscillations is considerably smaller in the simulated coherence. In principle, this means that the decrease in coherence cannot be solely attributed to the decorrelation caused by changes in soil moisture. However, it is important to note that the SM data were acquired at a depth of 15 cm, while the radar is sensitive to soil moisture in the first few centimeters of the ground. The dynamic range in soil moisture values is attenuated as the depth increases, and the influence of changes in air temperature, wind and air humidity disappears. As a possible solution, currently under evaluation, the SM right below the surface could be estimated from the actual SM data measured at 15 cm depth, thus enabling a more accurate comparison.

In addition to this, but not shown here due to space constraints, the VPD series oscillate daily, with low values during night time and an increase at dawn, as the temperature increases and the air can hold more water vapour. These oscillations again resemble the behaviour of the coherence time series.

4. CONCLUSIONS

The availability of sub-daily radar acquisitions has proved valuable for observing the sensitivity of SAR interferometry to short-time oscillations in soil moisture and features related to daily cycles in the vegetation, which could be relevant in various scientific fields, such as hydrology and agriculture. The rate of decorrelation has been studied at different stages of the growing season of a crop, as well as the daily oscillations of the coherence for sub-daily temporal baselines, which had not been observed before. The contribution of changes in soil moisture and evapotranspiration in these oscillations has been studied.

The results of this study are still being analysed and will be displayed at the conference. Future points of interest include:

- The estimation and validation of soil moisture right below the surface from the available 15 cm deep data.
- The study of the tendencies of the periodic cycle that coherence experiences during the season: rate of decorrelation, the amplitude of oscillation and the moment of the day where the minimum coherence value is reached.
- The effect of setting the primary image at different times during the day.
- A new campaign including both C and X-band, to profit from the combination of multiple frequencies.

5. REFERENCES

[1] Susan C. Steele-Dunne, Heather McNairn, Alejandro Monsivais-Huertero, Jasmeet Judge, Pang-Wei Liu, and Kostas Papathanassiou, "Radar remote sensing of agricultural canopies: A review," *IEEE Journal of Selected Topics in Applied Earth Observations and Remote Sensing*, vol. 10, no. 5, pp. 2249–2273, 2017.

[2] Richard Bamler and Philip Hartl, "Synthetic aperture radar interferometry," *Inverse Problems*, vol. 14, pp. R1–54, 01 1998.

[3] Mario Busquier, Juan M. Lopez-Sanchez, Alejandro Mestre-Quereda, Elena Navarro, María P. González-Dugo, and Luciano Mateos, "Exploring TanDEM-X interferometric products for crop-type mapping," *Remote Sensing*, vol. 12, no. 11, 2020.

[4] Alejandro Mestre-Quereda, Juan M. Lopez-Sanchez, Fernando Vicente-Guijalba, Alexander W. Jacob, and Marcus E. Engdahl, "Time-series of Sentinel-1 interferometric coherence and backscatter for crop-type mapping," *IEEE Journal of Selected Topics in Applied Earth Observations and Remote Sensing*, vol. 13, pp. 4070–4084, 2020.

[5] Tina Nikaein, Lorenzo Iannini, Ramses A. Molijn, and Paco Lopez-Dekker, "On the value of Sentinel-1 InSAR coherence time-series for vegetation classification," *Remote Sensing*, vol. 13, no. 16, 2021.

[6] Urs Wegmuller and Charles Werner, "Retrieval of vegetation parameters with SAR interferometry," *IEEE Transactions on Geoscience and Remote Sensing*, vol. 35, no. 1, pp. 18–24, 1997.

[7] Xavier Blaes and Pierre Defourny, "Retrieving crop parameters based on tandem ERS 1/2 interferometric coherence images," *Remote Sensing of Environment*, vol. 88, no. 4, pp. 374–385, 2003.

[8] Noelia Romero-Puig and J.M. Lopez-Sanchez, "A review of crop height retrieval using InSAR strategies: Techniques and challenges," *IEEE Journal of Selected Topics in Applied Earth Observations and Remote Sensing*, vol. 14, pp. 7911–7930, July 2021.

[9] Rouhollah Nasirzadehdizaji, Ziyadin Cakir, Fusun Balik Sanli, Saygin Abdikan, Antonio Pepe, and Fabiana Calò, "Sentinel-1 interferometric coherence and backscattering analysis for crop monitoring," *Comput. Electron. Agric.*, vol. 185, pp. 106118, 2021.

[10] Ankur Pandit, Surya Sawant, Jayantrao Mohite, and Srinivasu Pappula, "Sentinel-1-derived coherence time-series for crop monitoring in Indian agriculture region," *Geocarto International*, pp. 1–21, 2022.

[11] Arturo Villarroya-Carpio, Juan M. Lopez-Sanchez, and Marcus E. Engdahl, "Sentinel-1 interferometric coherence as a vegetation index for agriculture," *Remote Sens. Environ.*, vol. 280, pp. 113208, 10 2022.

[12] ESA, "Report for Assessment: Earth Explorer 10 Candidate Mission Hydroterra," Tech. Rep., European Space Agency, Noordwijk, The Netherlands, 2020, ESA-EOPSM-HYDRO-RP-3779, 131p.

[13] Susan C. Steele-Dunne et al., "A SAR Mission Concept for Sub-Daily Microwave Remote Sensing of Vegetation," Invited session 3D Microwave Remote Sensing of Vegetation, EUSAR, 2024.

[14] Albert R. Monteith and Lars M. H. Ulander, "A tower-based radar study of temporal coherence of a boreal forest at P-, L-, and C-bands and linear cross polarization," *IEEE Transactions on Geoscience and Remote Sensing*, vol. 60, pp. 1–15, 2022.

[15] Nadia Ouaadi, Lional Jarlan, Ludovic Villard, Adnane Chakir, Saïd Khabba, Pascal Fanise, Mohamed Kasbani, Zoubair Rafi, Valerie Le Dantec, Jamal Ezzahar, and Pierre-Louis Frison, "Temporal decorrelation of C-band radar data over wheat in a semi-arid area using sub-daily tower-based observations," *Remote Sensing of Environment*, vol. 304, pp. 114059, 2024.

[16] Albert Aguasca, Jordi Biscamps Dalmau, Xavier Fabregas, Jordi Llop Casamada, Jordi J. Mallorqui, Mireia Mas, and Hector Palacio, "HydroSoil - Ground based SAR experiments for soil moisture measurements," Tech. Rep., European Space Agency, 2020.

[17] Yu Morishita and Ramon F. Hanssen, "Temporal decorrelation in l-, c-, and x-band satellite radar interferometry for pasture on drained peat soils," *IEEE Transactions on Geoscience and Remote Sensing*, vol. 53, no. 2, pp. 1096–1104, 2015.

[18] Martti T. Hallikainen, Fawwaz T. Ulaby, Myron C. Dobson, Mohamed A. El-rayes, and Lil-kun Wu, "Microwave dielectric behavior of wet soil-part 1: Empirical models and experimental observations," *IEEE Transactions on Geoscience and Remote Sensing*, vol. GE-23, no. 1, pp. 25–34, 1985.

[19] Francesco De Zan, Alessandro Parizzi, Pau Prats-Iraola, and Paco López-Dekker, "A sar interferometric model for soil moisture," *IEEE Transactions on Geoscience and Remote Sensing*, vol. 52, no. 1, pp. 418–425, 2014.

[20] Roddy R. Rogers, *A short course in cloud physics*, Butterworth-Heinemann, Oxford; Boston, Third edition, 1989.